INTERNATIONAL JOURNAL FOR NUMERICAL METHODS IN FLUIDS
Int. J. Numer. Meth. Fluids 2000; **33**: 695–710

A two-scale low-Reynolds number turbulence model

Shenq-Yuh Jaw[a,*,1] and Robert R. Hwang[b]

[a] *Department of Naval Architecture, National Taiwan Ocean University, Keelung, Taiwan, Republic of China*
[b] *Institute of Physics, Academia Sinica, Taipei, Taiwan, Republic of China*

SUMMARY

In this study, a two-scale low-Reynolds number turbulence model is proposed. The Kolmogorov turbulence time scale, based on fluid kinematic viscosity and the dissipation rate of turbulent kinetic energy (ν, ε), is adopted to address the viscous effects and the rapid increasing of dissipation rate in the near-wall region. As a wall is approached, the turbulence time scale transits smoothly from a turbulent kinetic energy based (k, ε) scale to a (ν, ε) scale. The damping functions of the low-Reynolds number models can thus be simplified and the near-wall turbulence characteristics, such as the ε distribution, are correctly reproduced. The proposed two-scale low-Reynolds number turbulence model is first examined in detail by predicting a two-dimensional channel flow, and then it is applied to predict a backward-facing step flow. Numerical results are compared with the direct numerical simulation (DNS) budgets, experimental data and the model results of Chien, and Lam and Bremhorst respectively. It is proved that the proposed two-scale model indeed improves the predictions of the turbulent flows considered.

KEY WORDS: k–ε model; low-Reynolds number model; two-scale model

1. INTRODUCTION

The advancement of large computers has led to the wide use of higher-order turbulence closure models to predict turbulent flows. The most popular class includes the k–ε type turbulence models [1] in which the turbulent kinetic energy k and its dissipation rate ε are determined from two partial differential equations (PDEs). Reynolds stresses can be determined either from Reynolds stress models or from a Boussinesq eddy viscosity model,

$$-\overline{u_i u_j} = \nu_t\left(\frac{\partial U_i}{\partial x_j}+\frac{\partial U_j}{\partial x_i}\right)-\frac{2}{3}\delta_{ij}k$$

* Correspondence to: Department of Naval Architecture, National Taiwan Ocean University, Keelung 20224, Taiwan, Republic of China.
[1] E-mail: shjaw@na.ntou.edu.tw

Received February 1999
Revised May 1999

etc. Here v_t is the eddy viscosity, defined as $v_t = C_D(k^2/\varepsilon)$. With k and ε available, the turbulence length scale can then be determined from the relationship $k^{1.5}/\varepsilon$ based on dimensional analysis, and hence, unlike some simpler mixing length models, artificially introducing a turbulence length scale is not necessary. These models have been successfully applied in many engineering applications of high Reynolds number equilibrium turbulent flows [2].

When applying the $k-\varepsilon$ models to solve wall turbulent flows, certain near-wall modifications are required in the models since the rigid boundary will exert several different affects on turbulence [3]. Firstly, a wall will reduce the length scales of the fluctuation and raise the dissipation rate. Secondly, it will enforce a no-slip condition, thus ensuring that within a wall-adjacent sub-layer, turbulent stresses are negligible and viscous effects on transport processes become of vital importance. Thirdly, a wall will also reflect pressure fluctuations, thereby inhibiting the transfer of turbulence energy into fluctuations normal to the wall. Under such conditions, the high-Reynolds number turbulence models are no longer valid and cannot be applied directly to predict the near-wall turbulent flows, unless appropriate near-wall modifications are adopted.

Wall functions [4] are one of the well-known near-wall modifications. The so-called wall functions relate surface boundary conditions to points in the fluid away from the boundaries and thereby avoid the problem of modelling the direct influence of viscosity. The validity of this procedure is, of course, restricted to situations in which the Reynolds number is sufficiently high for the viscous effects to be unimportant or where universal wall functions are well established. As a result, the wall functions are not very suitable for turbulent flows with such complexities as adverse pressure gradient, streamline curvature or complex three-dimensional flows and so forth.

Predicting turbulent wall shear flows directly from a wall is attractive from a practical standing point [5]. Since the momentum and continuity equations are solved up to the wall, it provides the means to include the complexities of complex turbulent flows without invoking wall functions. Over the past years, many suggestions have been made for both Reynolds stress models and eddy–viscosity models to extend their use at low Reynolds numbers and to describe the flow close to a solid wall. The extensions all involve modifying the viscous diffusion, dissipation and, for Reynolds stress models, the pressure redistribution [3]. Damping functions and *ad hoc* modifications are required to modify their near-wall behaviour.

The necessity of employing different kinds of near-wall modifications is due to the fact that most of the near-wall turbulence models in use are derived based on the concept of single turbulence scale. For instance, the length and time scales of turbulence are characterized by k and ε only. The turbulence scales determined from (k, ε) are known to characterize the energy containing large turbulent eddies. They are not the appropriate scales to describe the dissipation dominated near-wall turbulence. Therefore, various forms of near-wall modifications have been proposed, however, without producing consistent near-wall predictions. Reviews of near-wall turbulence models can be found in Patel *et al.* [6] and So *et al.* [7].

An alternative and physically more realistic way to model the near-wall turbulence is to introduce the Kolmogorov turbulence scale in the dissipation dominated near-wall region [8,9]. The Kolmogorov scale, based on (ε, v), provides turbulence models with a proper lower bound as the wall is approached, since none of them will become zero on the wall. Employing the Kolmogorov scale in a low-Reynolds number turbulence model at least properly addresses the

first two wall effects mentioned above, namely, the viscous effects and the rapid increasing of turbulence dissipation. It is thus expected that adopting both the (k, ε) and (ε, v) scales in the same turbulence model, allowing them to transit smoothly from the former to the latter one, will improve the model performance. Furthermore, damping functions or *ad hoc* modifications may also be simplified with the appropriate near-wall turbulence scale adopted. A two-scale low-Reynolds number turbulence model is thus proposed. The proposed model is first examined by predicting a two-dimensional turbulent channel flow [10] and then it is applied to predict a backward-facing step flow [11]. Numerical results are compared in detail with the direct numerical simulation (DNS) budgets, experimental data and the model results of Chien [12] and Lam and Bremhorst [13], the better ones evaluated by Patel *et al.* [6]

2. NEAR-WALL TURBULENCE MODELS

The steady, incompressible Navier–Stokes equations for turbulent flow can be written as

$$U_j \frac{\partial U_i}{\partial X_j} = -\frac{1}{\rho}\frac{\partial P}{\partial X_i} + \frac{\partial}{\partial X_j}\left(v\frac{\partial U_i}{\partial X_j}\right) - \frac{\partial \overline{u_i u_j}}{\partial X_j} \tag{1}$$

$$\frac{\partial U_i}{\partial X_i} = 0 \tag{2}$$

The parameters U_j and u_j represents mean and fluctuating velocities in the j-direction respectively, P is the static pressure, ρ is the fluid density, v is the fluid kinematic viscosity, and the overbarred quantities $\overline{u_i u_j}$ are the Reynolds stresses. Since there are more unknowns than equations available the problem is not closed. Therefore, it is necessary to introduce k, ε or even the Reynolds stress $\overline{u_i u_j}$, into the transport equations to meet the requirement that the number of unknowns is equal to the number of equations available and close the problem.

For the low-Reynolds number, eddy–viscosity models, Reynolds stresses are determined from the algebraic Boussinesq eddy–viscosity model. A general form of the corresponding transport equations can be written as

$$-\overline{u_i u_j} = v_t\left(\frac{\partial U_i}{\partial X_j} + \frac{\partial U_j}{\partial X_i}\right) - \frac{2}{3}\delta_{ij}k \tag{3}$$

$$v_t = C_D f_\mu T k$$

$$\varepsilon = \bar{\varepsilon} + D$$

$$\frac{Dk}{Dt} = \frac{\partial}{\partial X_l}\left[C_k f_\mu T k \frac{\partial k}{\partial X_l} + v\frac{\partial k}{\partial X_l}\right] + P_k - \varepsilon \tag{4}$$

$$\frac{D\bar{\varepsilon}}{Dt} = \frac{\partial}{\partial X_l}\left[C_\varepsilon f_\mu T k \frac{\partial \bar{\varepsilon}}{\partial X_l} + v\frac{\partial \bar{\varepsilon}}{\partial X_l}\right] + C_{\varepsilon 1} f_1 \frac{1}{T} P_k - C_{\varepsilon 2} f_2 \frac{1}{T}\bar{\varepsilon} + E \tag{5}$$

Here D is chosen such that the numerical boundary condition is $\bar{\varepsilon} = 0$ at the wall. The additional empirical term E is introduced to increase the growth of ε with wall distance if f_1 is set to be unity. T is the time scale, defined as

$$T = \max\left(\frac{k}{\varepsilon},\ C_T\left(\frac{\nu}{\varepsilon}\right)^{1/2}\right)$$

for the proposed two-scale model, with $C_T = 6$. The coefficient C_T is adopted directly from the work of Durbin [9] by reference to DNS data, and is shown to produce the correct near-wall ε distribution in this study. The time scale becomes k/ε far from the boundaries. Near a wall, the time scale becomes the Kolmogorov dissipation scale $C_T(\nu/\varepsilon)^{1/2}$, which is a suitable lower bound on T. For the low-Reynolds number models of Chien [12] and Lam and Bremhorst [13], T is kept to be k/ε all the way down to the wall. The parameter P_k is the production term,

$$P_k = -\overline{u_i u_j}\frac{\partial U_i}{\partial X_j}$$

Wall effects are approximated using damping functions f_μ, f_1 and f_2. Wall damping functions, boundary conditions and model coefficients for the proposed two-scale model and the model of Chien [12] and Lam and Bremhorst [13] are listed in Table I. It should be pointed out that in the proposed two-scale model, f_1 is expressed in terms of the ratio of turbulence production over dissipation. It is not a damping function but a modification to the $C_{\varepsilon 1}$ model coefficient. Since f_2 equals unity, f_μ is the only damping function required in the proposed model.

Some dimensionless parameters appearing in Table I are defined as

$$R_T = \frac{k^2}{\nu\bar{\varepsilon}}, \qquad R_y = \frac{\sqrt{k}y}{\nu}, \qquad y^+ = \frac{yu_\tau}{\nu}, \qquad u_\tau = \sqrt{\frac{\tau_w}{\rho}}$$

Note also that the damping function f_μ of Lam and Bremhorst's model [13] is expressed in terms of R_y and R_T, which are defined as a function of k. Since turbulent kinetic energy k is always positive, R_y and R_T are always positive and will not alter their sign when reverse flow occurs. To preserve such an advantage, the damping functions adopted in the proposed two-scale model also include these parameters.

3. PREDICTION OF FULLY DEVELOPED TURBULENT CHANNEL FLOW

DNS of turbulent channel flows provide a complete database to develop and test turbulence models. To investigate in detail the performance of the near-wall turbulence models considered in this study, the low-Reynolds number DNS channel flow of Kim *et al.* [10] is solved directly from the wall. Both the mean quantities and the budgets of each modelling term of the k and ε transport equations are compared. The simulated flow fields are for a channel flow at a Reynolds number $Re_\tau = u_\tau\delta/\nu = 180$ based on ν, the wall shear velocity u_τ and the channel half-width δ. This corresponds to a Reynolds number $Re = U_c\delta/\nu = 3200$ based on the mean centreline velocity U_c and channel half-width δ.

Table I. Low-Reynolds number models

(a) Damping functions and near-wall modifications

Authors	f_μ	f_1	f_2	E
Jaw and Hwang	$[1-\exp(-0.0165R_y)]^2\left(1+\frac{20.5}{R_T}\right)$ or $\left[1-\exp\left(-\frac{R_y}{70}\right)\right]^{1.75}$	$[1+0.1(P/\varepsilon)]$	1	0
Lam and Bremhorst	$[1-\exp(-0.0165R_y)]^2\left(1+\frac{20.5}{R_T}\right)$	$1+\left(\frac{0.05}{f_\mu}\right)^3$	$1-\exp(-R_T^2)$	0
Chien	$1-\exp(-0.0115y^+)$	1	$1-0.22\exp\left(-\frac{R_T}{6}\right)^2$	$-2\nu\left(\frac{\bar{\varepsilon}}{y^2}\right)\exp(-0.5y^+)$

(b) Model coefficients and boundary conditions

Authors	D	$\bar{\varepsilon}_w$—B.C.	C_D	C_k	C_ε	$C_{\varepsilon 1}$	$C_{\varepsilon 2}$	$C_{\varepsilon 3}$
Jaw and Hwang	0	$2\nu\left(\frac{\partial\sqrt{k}}{\partial y}\right)^2$	0.09	0.09	0.07	1.44	1.92	
Lam and Bremhorst	0	$\nu\frac{\partial^2 k}{\partial y^2}$	0.09	0.09	0.07	1.44	1.92	
Chien	$2\nu\frac{k}{y^2}$	0	0.09	0.09	0.07	1.35	1.8	

For a two-dimensional, fully developed turbulent flow, the Navier–Stokes equations, incorporated with the low-Reynolds number turbulence model, can be written as

$$\nu\frac{\partial U}{\partial y}-\overline{uv}=\frac{y}{\delta}u_\tau^2 \tag{6}$$

$$-\overline{uv}=\nu_t\frac{\partial U}{\partial y},\qquad \nu_t=C_D f_\mu kT$$

$$T=\max\left(\frac{k}{\varepsilon},\ C_T\left(\frac{\nu}{\varepsilon}\right)^{1/2}\right),\qquad C_T=6$$

$$\frac{Dk}{Dt}=\frac{\partial}{\partial y}\left[(\nu_t+\nu)\frac{\partial k}{\partial y}\right]+\nu_t\left(\frac{\partial U}{\partial y}\right)^2-\varepsilon \tag{7}$$

$$\frac{\mathrm{D}\varepsilon}{\mathrm{D}t}=\frac{\partial}{\partial y}\left[\left(\frac{\nu_t}{1.3}+\nu\right)\frac{\partial\varepsilon}{\partial y}\right]+C_{\varepsilon 1}f_1\frac{1}{T}\nu_t\left(\frac{\partial U}{\partial y}\right)^2-C_{\varepsilon 2}f_2\frac{1}{T}\varepsilon \tag{8}$$

Note that in Equation (8), the Kolmogorov time scale has no effect for the production term $C_{\varepsilon 1}$, since the reciprocal of the time scale is eliminated by the time scale of the eddy viscosity.

For a fully developed flow, $\mathrm{D}/\mathrm{D}t=0$, the above equations are simplified to ordinary differential equations (ODEs). From Equation (6) it is known that given u_τ, the mean velocity and all the turbulence quantities can be found from integrating Equations (6)–(8). The value of u_τ is found to be 0.05625 from the conditions that $Re_\tau=u_\tau\delta/\nu=180$ and $Re=U_c\delta/\nu=3200$. Since the flow is symmetric to its centreline, the symmetrical boundary conditions,

$$\frac{\mathrm{d}\varepsilon}{\mathrm{d}y}=\frac{\mathrm{d}k}{\mathrm{d}y}$$

are applied at $y=\delta$. At $y=0$, the wall conditions are $U=k=0$. The wall conditions of ε for different models are listed in Table I(b).

Sixty non-uniform nodes are distributed within the channel half-width, and transport equations are discretized using finite volume method (FVM) [14]. Specifying appropriate boundary conditions, all the transport differential equations can be solved in a similar way. To check if the solution has reached grid independence, 40 and 80 non-uniform nodes are also adopted to solve the DNS channel flow using the two-scale model. It is found that, for such a low-Reynolds number turbulent flow, the solutions of 40 and 80 nodes are almost identical in the case when the near-wall grids are properly distributed. Therefore, a compromise of 60 nodes is used throughout the study, with 14 nodes within $y^+\leq 5$ and 24 nodes within $5\leq y^+\leq 40$. The convergence criterion is specified as the relative error of all variables being smaller than 1×10^{-5}. Different time step and relaxation factors are adopted for different models. Discussions of numerical convergence are not presented here since it is not the purpose of the present study.

4. COMPARING WITH THE DNS BUDGETS

The major difference between the proposed two-scale model and the other two low-Reynolds number models is on the determination of turbulence time scale. Figure 1 compares the time scale distribution for k/ε and the Kolmogorov time scale $C_T\sqrt{\nu/\varepsilon}$ with $C_T=6$, over the range $0\leq y^+\leq 40$. This figure shows that the cross of time scale occurs in the viscous sub-layer, at $y^+\cong 7$. Different C_T values, $3\leq C_T\leq 12$, were also tested, which resulted in only a little difference of the near-wall time scale variations. Therefore, the predicted results are considered insensitive to the different C_T values. It should also be remarked that the kink at the cross of the time scale does not have any significant influence, since the difference between the kink and its linear distribution is small. Besides, when determining the eddy viscosity, the time scale is multiplied by f_μ, the kink falls within the range where $f_\mu T$ is approximately equal to zero, as shown in Figure 1.

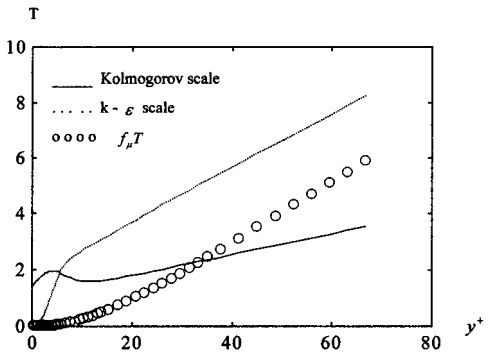

Figure 1. Time scale distribution.

Specifying the shear velocity $u_\tau = 0.05625$, the integrated $-\overline{uv}^+$ distribution is shown in Figure 2. The symbol '○' represents the DNS data picked from Kim *et al.* [10]. Model results are represented by the different symbols of lines shown in the figure. It is found that the proposed two-scale model predicts the overall best Reynolds stress distribution. The other two models predict either a better near-wall or peak Reynolds stress distribution, while deviating from the DNS results for the other parts.

Equation (6) indicates that, with u_τ specified, the velocity distribution of a fully developed flow is mainly influenced by the Reynolds stress $-\overline{uv}$. If the adopted turbulence model can not predict correctly the $-\overline{uv}$ distribution, the integrated mean velocity profile will also deviates from the DNS results. This is found to be true by comparing the model results with the DNS data. As shown in Figure 3, only the mean velocity profile obtained from the two-scale model fits precisely with the DNS results, the other two velocity distributions contain certain discrepancies. Figure 4, the log-law distribution of mean velocities, shows the same tendency. Note that mean velocities are integrated by specifying constant wall shear stress; the near-wall velocities predicted from different turbulence models are almost identical. However, away from the wall the velocity profiles are diverse.

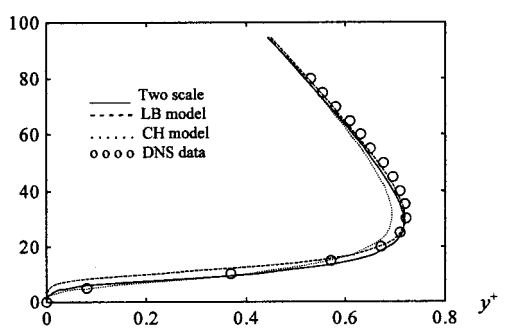

Figure 2. Reynolds stress distribution.

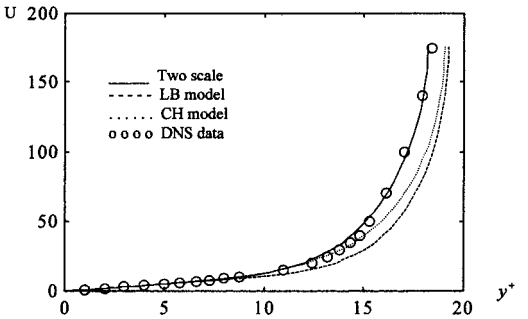

Figure 3. Mean velocity distribution.

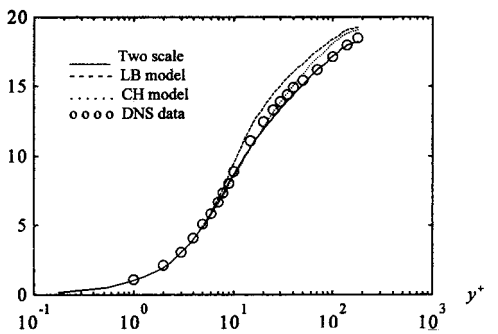

Figure 4. Log-law distribution of velocity.

To evaluate turbulence models in detail, the budget of each modelling term of the k, ε transport equations are also examined. Figure 5 presents the modelled k budget compared with the DNS results of exact turbulent kinetic energy equation. For the turbulent diffusion, $(\partial/\partial y)[C_k Tk(\partial k/\partial y)]$ and the production $P_k = -\overline{uv}(\partial U/\partial y)$ terms, all the models can predict correctly the trend as the DNS results, even though their peak values and peak positions have some differences, as shown in Figure 5(a) and (b) respectively. As for the viscous diffusion $(\partial/\partial y)[v(\partial k/\partial y)]$ and dissipation budget of k, Figure 5(c) and (d) show that only the two-scale model predicts correctly the near-wall distribution with its peak value on the wall. For the dissipation budget, all the other models predict only a single peak, located close to $y^+ \approx 16$ with their values in between the two peaks of the DNS results.

It should be remarked that several different ε wall boundary conditions have been tested with the two-scale model. However, only the form

$$\varepsilon_w = 2v\left(\frac{\partial\sqrt{k}}{\partial y}\right)^2$$

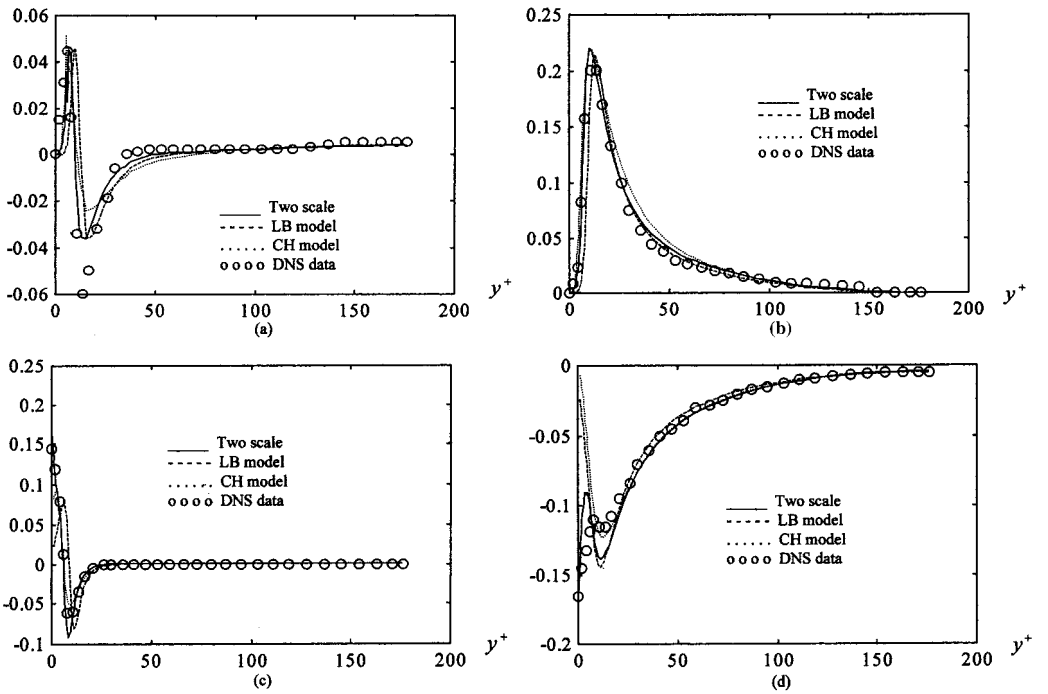

Figure 5. Budgets of turbulent kinetic energy. (a) Turbulent diffusion; (b) production; (c) viscous diffusion; (d) dissipation.

gives the correct wall value and the proper coefficient for the linear term as well, which in turn renders the correct near-wall ε distribution. Some respective proponents also manifest that such an ε distribution can also be reproduced by using complex damping functions and *ad hoc* near-wall modifications [15,16]. However, too many *ad hoc* modifications generally diminish the flexibility of the model application and sometimes will also bring about the numerical stability problem. Since introducing the Kolmogorov scale simplifies, but not sophisticates, the near-wall turbulence modelling, it seems to be the better way as improving the near-wall turbulence prediction is considered.

It should also be pointed out that in the k equation only the turbulent diffusion term requires a model and as shown in Figure 5(a) the differences between modelled turbulent diffusion and the DNS results are small. The k equation is thus considered to be relatively accurate so that prediction of k directly from wall can be achieved without any modification. No evidence indicates that the main difficulty of turbulence predictions is arisen from the turbulent diffusion model.

Figure 6 presents the budgets of the modelled ε equation. According to Mansour *et al.* [17], the viscous diffusion and destruction terms of the ε equation are better modelled together. Figure 6(a) compares the summation of these two terms,

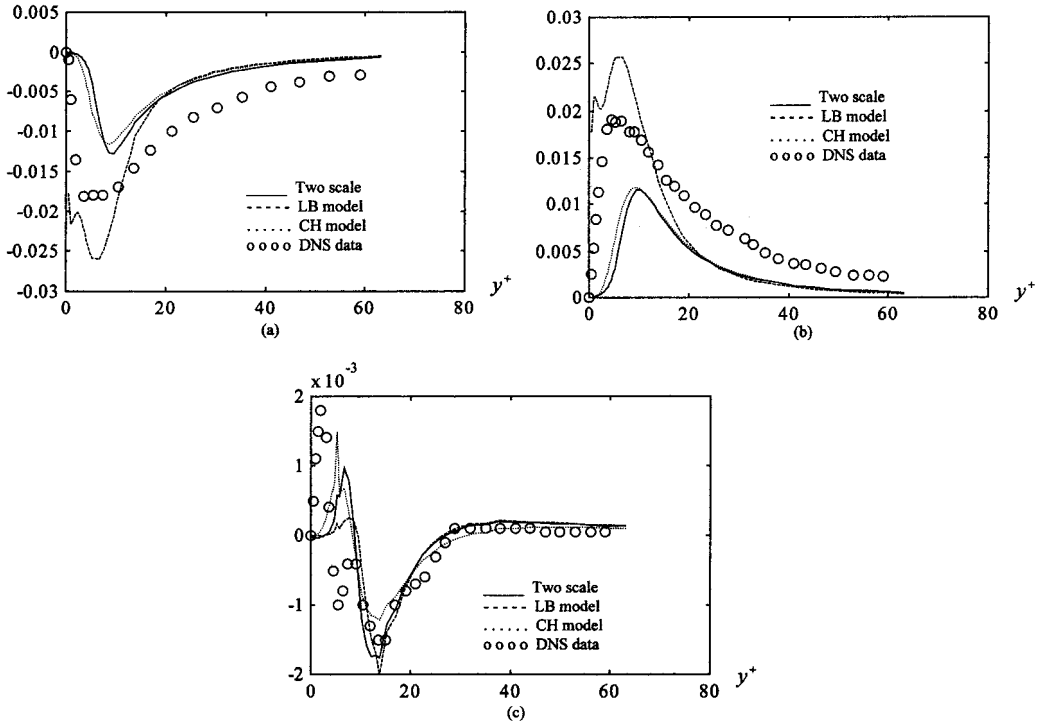

Figure 6. Budgets of kinetic energy dissipation. (a) Viscous diffusion + destruction; (b) production; (c) turbulent diffusion.

$$\frac{\partial}{\partial y}\left(\nu \frac{\partial \varepsilon}{\partial y}\right) - C_{\varepsilon 2} f_2 \frac{1}{T}\varepsilon$$

Figure 6(b) shows the modelled production

$$C_{\varepsilon 1} f_1 \frac{1}{T} \nu_t \left(\frac{\partial U}{\partial y}\right)^2$$

versus the production terms of the exact equation. Obviously, none of the models predicts the correct results. However, it is found that the discrepancies between model results and DNS data of these two figures are similar in magnitude but opposite in sign. Summing these terms together, the discrepancies will be eliminated by each other and the model results would fit much better to the DNS data. Their accuracy can even be evaluated from examining the distribution of turbulent diffusion,

$$D_\varepsilon^t = \frac{\partial}{\partial y}\left(C_\varepsilon T k \frac{\partial \varepsilon}{\partial y}\right)$$

For a fully developed flow, the convective terms vanish. The summation of viscous diffusion, turbulent diffusion, production and destruction terms equals zero, or equivalently the summation of viscous diffusion, production and destruction is equal to the negative of turbulent diffusion. Since the magnitude of turbulent diffusion is one order smaller than the magnitude of the other modelling terms, as shown in Figure 6(c), the overall prediction accuracy of the ε equation is much better than its individual modelling term. This may explain why, even using such an inaccurately modelled ε equation, one can still predict satisfactorily some simple turbulent flows.

The inconsistency of the model results with the DNS budgets may imply that the modelling of the ε equation is incomplete. The ε equation is known to be the most inaccurately modelled equation in the k–ε type turbulence models since each term on the right-hand side of its exact transport equation requires a model [4]. What is worse is the physical meaning of some of those terms is not clearly understood, hence they were simply dropped or simplified when modelling the ε equation. Adopting the Kolmogorov scale or even using higher-order Reynolds stress turbulence models [18] will not improve too much the performance of each individual modelling term. Reconsidering the modelling philosophy of the ε equation seems necessary.

Equations (6)–(8) show that, with k, ε transport equations fixed in their two-scale form, and wall shear stress specified, the integrated mean velocity is mainly influenced by the Reynolds stress $-\overline{uv}$ distribution, or equivalently, the f_μ damping function. Several f_μ damping functions [4] were tested. It is found that only the f_μ of Lam and Bremhorst's model [13] does not require a modification and renders the best results directly. Since f_μ is the only damping function required in the proposed model, if different forms of the f_μ function were modified to yield the same mean velocity distribution, all the predicted turbulence transport quantities, and their budgets will be almost identical. Figure 7 demonstrates one such example that, by modifying the f_μ from a two-layer model [19] to be

$$f_\mu = \left[1 - \exp\left(-\frac{R_y}{70}\right)\right]^{1.75}$$

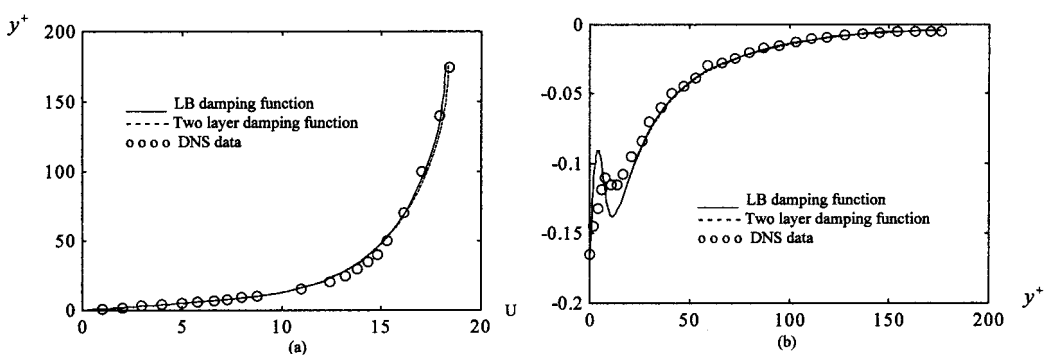

Figure 7. Results obtained from two different damping functions. (a) Mean velocity; (b) dissipation.

the predicted results from two different damping functions are consistent and almost identical. Using such characteristics, a simpler form of the f_μ damping function can be derived to ease the numerical computation without deteriorating the prediction accuracy.

5. PREDICTION OF BACKWARD-FACING STEP FLOW

The backward-facing step flow is a fundamental configuration of internal flows and has been extensively studied. The flow separates at the step, reattaches at downstream and then recirculates behind the step, which provides turbulence models with additional test domain. Prediction of such a flow can thus enable one to examine the model capability in predicting not only the distribution of turbulence transport quantities but also the mean velocity distribution. However, when reverse flow occurs, adopting a model whose damping function relates directly to wall shear stress, such as the model of Chien [12], is not appropriate. Hence, only the proposed two-scale model and the model of Lam and Bremhorst [13] are adopted here.

The configuration of the flow considered is the same as that of the experimental set-up of Smyth [11], as shown in Figure 8. The dimensionless downstream channel half-height is $W = 1$, the upstream channel half-height is $H = \frac{2}{3}$ and the step height is $\frac{1}{3}$. W is chosen as the reference length scale and the mean inlet velocity U_m is the reference velocity scale. Based on these scales, the Reynolds number is 30210 and the expansion ratio, defined as W/H, is 1.5. The turbulent flow is steady and the separation is symmetric. Therefore, only the upper half of the backward-facing step channel flow is considered in this numerical calculation. The distance between the inlet and the step is taken to be 1.5 and the outlet is 12 units downstream from the step. Cartesian co-ordinates are used with the X-axis directed along the centreline and the origin is located at the step.

The inlet profiles of U, k, ε were not provided by Smyth's experiment [11]. They are determined empirically such that the predicted results match closely with Smyth's experimental data [11] of U at the step entrance, $X = 0$. Several inlet profiles were examined. The following profiles are selected for all the calculations:

$$U_i = 1.17(1 - Y)^{1/7}$$

$$k_i = 0.15(0.023 + 0.19Y - 0.799Y^2 + 1.335Y^3)$$

$$\varepsilon = 1.2k_i^{3/2}$$

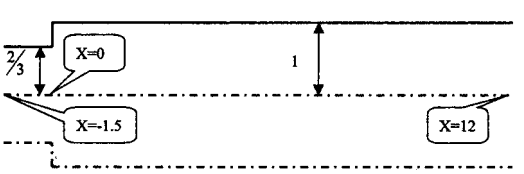

Figure 8. Configuration of backward-facing step flow.

For the rest of the boundaries, wall, symmetric and fully developed outlet conditions are specified.

A grid independence study is performed first. Three different node distributions, namely 68×62, 102×62 and 102×89 nodes, are adopted to predict the backward-facing step flow using Lam and Bremhorst's model [13]. For the longitudinal, 68 nodes distribution, the grid spacing ranges from 0.01 to 0.4, while for the 102 nodes distribution, it is from 0.006 to 0.2. In the vertical direction, the grid spacing is from 0.002 to 0.07 and 0.0012 to 0.05 for the 62 and 89 nodes distribution respectively. The convergence criterion is specified the same as that of the DNS channel flow. However, different time steps and relaxation factors are adopted at different time marching stages. Discussions of numerical convergence are not presented since it is not the purpose of the present study. Figure 9 shows some of the predicted profiles. It is found that if the nodes are properly distributed in the critical region, such as the separation zone where flow characteristics are examined, the predicted results are almost identical and grid independence is reached. Hence, in the following discussion, only the solutions obtained from the 102×89 nodes are presented.

The velocity profile at the step entrance is checked first. Figure 10 shows that both turbulence models predict fairly close U profiles at the step entrance, and thus comparisons at downstream sections are meaningful. Note also that the advantage of adopting the near-wall Kolmogorov scale is clearly manifested in this figure. The two-scale model predicts a smaller near-wall velocity distribution, which fits closer to the experimental data.

Figure 11 compares the shear stress distribution along the bottom, starting from the corner of the step to the exit, of the channel. The positive shear stress appeared on the step corner implying that both models predict a tiny, secondary separation bubble right on the step corner. Note also that adopting the Kolmogorov scale in the near-wall region will increase the wall shear stresses, which in turn will shorten the predicted reattachment length of the separation flow. This is further confirmed in what is presented in the following. Comparisons of mean velocity U, turbulent kinetic energy k and Reynolds stress $(\overline{u^2})^{1/2}$ at the cross-section $X = 1.2$,

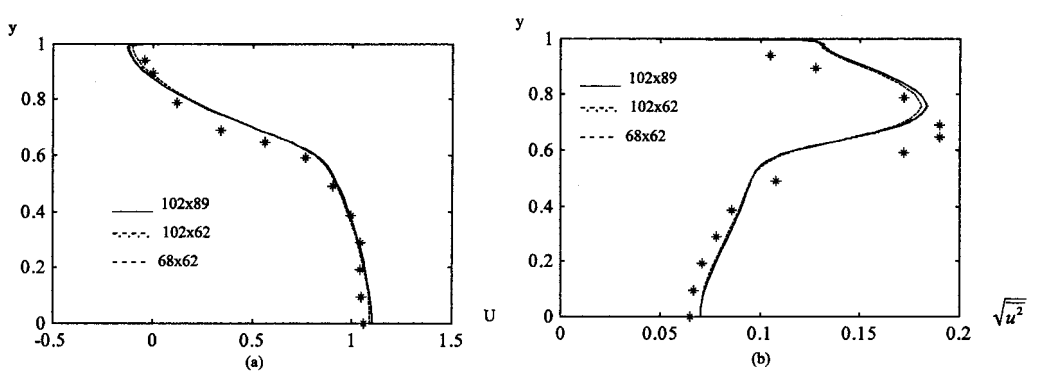

Figure 9. Grid independence examination. (a) Velocity profile at $X = 1.2$; (b) Reynolds stress $\sqrt{u^2}$ at $X = 1.2$.

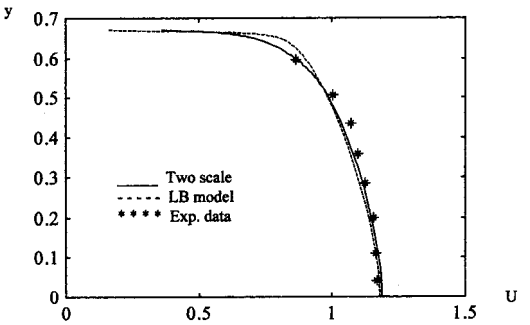

Figure 10. Velocity profile at step entrance.

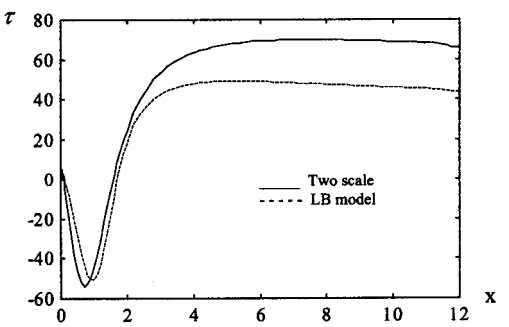

Figure 11. Wall shear stress distribution.

close to the end of the recirculation zone, are presented in Figure 12. Obviously, the two-scale model predicts better results. Figure 12(a) shows that the predicted reverse flow of the two-scale model matches closely with the experimental data. Checking the computational results, it is found that the predicted reattachment length extends to $X = 1.64$ and 1.77 for the two-scale model and the model of Lam and Bremhorst [13] respectively, while the experiments showed that $X = 1.5$. For the k and $(\overline{u^2})^{1/2}$ distributions, the two-scale model also renders better results than the model of Lam and Bremhorst [13]. However, certain discrepancies are still observed with experimental data, which is probably due to the limitations established in the eddy–viscosity type turbulence models that Reynolds stresses are approximated by the simple eddy–viscosity model. To further improve the prediction accuracy, adopting higher-order closure turbulence models, such as the second-order closure turbulence models [2], is required.

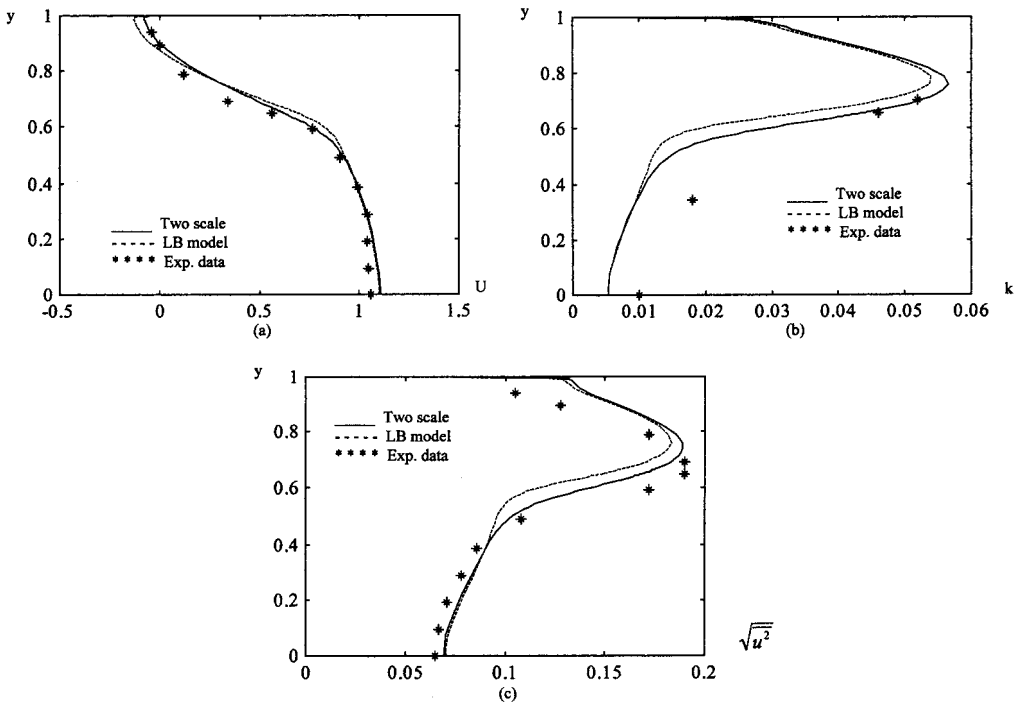

Figure 12. Prediction of backward-facing step flow. (a) Mean velocity at $X = 1.2$; (b) turbulent kinetic energy; (c) Reynolds stress $\sqrt{u^2}$ at $X = 1.2$.

6. CONCLUSIONS

Currently, there are many low-Reynolds number turbulence models available. However, the development of those models tends to sophisticate the damping functions and *ad hoc* modifications, which in turn deteriorates numerical stability and hampers the model applicability. A better way to improve the model performance would be simplifying the model form by introducing a physically realistic turbulence scale in the near-wall region. This is accomplished in the proposed two-scale low-Reynolds number turbulence model.

Adopting the second, Kolmogorov, turbulence scale in the near-wall region at least properly addresses two of the wall effects, namely the viscous effects and the rapid increasing of dissipation rate. In addition, the two-scale model simplifies, but not sophisticates, the damping functions and *ad hoc* modifications. Only the f_μ damping function is required in the proposed model. With appropriate boundary conditions specified, some related near-wall turbulence characteristics, such as the viscous diffusion, dissipation or velocity distributions, can be correctly reproduced. Sensitivity tests show that varying the time scale model coefficient, C_T, will not have a significant influence on the predicted results. Furthermore, if different forms of the f_μ function were modified to yield the same mean velocity distribution, all the predicted

turbulence transport quantities and their budgets will be almost identical. Using such characteristics, a simpler form of the f_μ damping function can be derived to ease the numerical computation without deteriorating the prediction accuracy.

The proposed two-scale turbulence model is first examined in detail by predicting a two-dimensional channel flow, and then applied to predict a backward-facing step flow. Numerical results are compared with the DNS budgets, experimental data and the model results of Chien [12] and Lam and Bremhorst [13] respectively. It is concluded that the two-scale low-Reynolds number turbulence model indeed improves the prediction of the turbulent flows considered.

REFERENCES

1. Jaw SY, Chen CJ. Present status of second order closure turbulence models, I: overview. *Journal of Engineering Mechanics* 1998; **124**(5): 485–501.
2. Jaw SY, Chen CJ. Present status of second order closure turbulence models, II: application. *Journal of Engineering Mechanics* 1998; **124**(5): 502–512.
3. Launder BE. Second-moment closure: present . . . and future? *International Journal for Heat and Fluid Flow* 1989; **10**(4): 282–300.
4. Chen CJ, Jaw SY. *Fundamentals of Turbulence Modeling*. Taylor & Francis: Washington, DC, 1998.
5. Jaw SY, Hwang RR. Prediction of turbulent wall shear flows directly from wall. *International Journal for Numerical Methods in Fluids* 1994; **19**(10): 869–888.
6. Patel VC, Rodi W, Scheuerer G. Turbulence models for near-wall and low Reynolds number flows: a review. *American Institute of Aeronautics and Astronautics Journal* 1984; **23**(9): 1308–1319.
7. So RMC, Lai YG, Zhang HS. Second-order near-wall turbulence closures: a review. *American Institute of Aeronautics and Astronautics Journal* 1991; **29**(11): 1819–1835.
8. Jaw SY, Chen CJ. Development of turbulence model including fractal and Kolmogorov scale. Symposium on Advances and Applications in Computational Fluid Dynamics, Winter Annual Meeting, American Society of Mechanical Engineers, Dallas, TX, 25–30 November, 1990.
9. Durbin PA. A Reynolds stress model for near-wall turbulence. *Journal of Fluid Mechanics* 1993; **249**: 465–498.
10. Kim J, Moin P, Moser R. Turbulence statistics in fully developed channel flow at low Reynolds number. *Journal of Fluid Mechanics* 1987; **177**: 133–166.
11. Smyth R. Turbulence flow over a plane symmetric sudden expansion. *Journal of Fluids in Engineering* 1979; **101**: 348–353.
12. Chien KY. Predictions of channel and boundary-layer flows with a low-Reynolds number turbulence model. *American Institute of Aeronautics and Astronautics Journal* 1982; **20**(1): 33–38.
13. Lam CKG, Bremhorst K. A modified form of the k–ε model for predicting wall turbulence. *Transactions of the American Society of Mechanical Engineers* 1981; **103**: 456–460.
14. Patankar SV. *Numerical Heat Transfer and Fluid Flow*. Hemisphere (McGraw-Hill): New York, 1980.
15. So RMC, Zhang HS, Speziale CG. Near-wall modeling of the dissipation rate equation. *American Institute of Aeronautics and Astronautics Journal* 1991; **29**(12): 2069–2076.
16. Nagano Y, Shimada M. Rigorous modeling of dissipation rate equation using direct simulation. *Japan Society of Mechanical Engineers International Journal Series B* 1995; **38**: 51–59.
17. Mansour NN, Kim J, Moin P. Reynolds-stress and dissipation rate budgets in a turbulent channel flow. *Journal of Fluid Mechanics* 1988; **194**: 15–44.
18. Jaw SY, Hwang RR. On the study of near wall behavior of k–ε turbulence models. *The Chinese Journal of Mechanics* 1998; **13**(3): 265–276.
19. Chen HC, Patel VC. Near-wall turbulence models for complex flows including separation. *American Institute of Aeronautics and Astronautics Journal* 1988; **26**: 641–648.

